Journal of Molecular Structure 994 (2011) 392–402

Contents lists available at ScienceDirect

Journal of Molecular Structure

journal homepage: www.elsevier.com/locate/molstruc

# Synthesis and structural characterization of amino acid and peptide derivatives featuring *N*-(*p*-bromobenzoyl) substituents as promising connection unit for bio-inspired hybrid compounds

Frank Eißmann, Edwin Weber *

*Institut für Organische Chemie, Technische Universität Bergakademie Freiberg, Leipziger Str. 29, D-09596 Freiberg/Sachsen, Germany*

ARTICLE INFO

*Article history:*
Received 23 February 2011
Received in revised form 23 March 2011
Accepted 24 March 2011
Available online 30 March 2011

*Keywords:*
*N*-(*p*-bromobenzoyl) amino acid
*N*-(*p*-bromobenzoyl) peptide
X-ray crystal structure
Hydrogen bonding
Strand packing motif
Peptide sheet structure

ABSTRACT

Using a sequence of activation, blocking and peptide coupling procedures, a series of ten amino acid and peptide derivatives **1**–**6** (**a**, **b**, respectively) featuring a *p*-bromobenzoyl substituent attached to the amino group of the parent compound has been synthesized. X-ray crystal structures of two corresponding amino acid (**1a**, **1b**), two amino acid ester (**3a**, **3b**) and three peptide ester derivatives (**4a**, **4b**, **5b**) are reported, with the amide and peptide bonds of the molecules all being planar and *trans* configurated. Intramolecular interactions dominating the packing motifs and thus giving rise to the formation of strands (**1a**, **3a**, **3b**, **4a**, **4b**), molecular pairs (**1b**) or sheets (**5b**) derive from N–H···O contacts, being further assisted by O–H···O and weaker C–H···O interactions, while bromo involved contacts are of minor importance.



## 1. Introduction

Being an interesting category of biomolecules, amino acids and peptides are extensively studied with regard to applications in the assembly of bio-inspired hybrid materials and nanotechnological devices [1,2]. Thus, functionalized, non-natural amino acids and peptides are of unbroken interest as they are essential building blocks for the construction of bioconjugates being comprised of synthetic molecules and amino acid or peptide fragments covalently linked to each other [3]. For a specific construction of bioconjugate materials, potential building blocks require functional groups allowing a chemoselective covalent bond formation between the components of the desired conjugate structure. Very attractive methods for this kind of bond formation are, among others, $Pd^0$ catalyzed cross-couplings or cycloaddition reactions [4]. For these types of reactions, halogenated compounds with the halogen substituent linked to a $sp^2$ carbon atom play a decisive role as corresponding building units or respective precursors. In the case of modern $Pd^0$ catalyzed C–C coupling reactions, comprising the methods originally developed by Sonogashira and Hagihara, Suzuki, Stille or Negishi [5], aryl halides can serve as one of the coupling components or can be further converted to terminal aryl acetylenes, aryl boronic acid derivatives, aryl stannanes and organozinc halides, being the second necessary building block for the coupling reactions mentioned above, respectively. Aryl halide derivatives are also important precursors for 1,3-dipolar Huisgen type cycloadditions, recently undergoing a revival referred to as "click" reactions [6], as they can easily be converted to the corresponding terminal aryl acetylene compounds [7] or to aryl azides [8]. In the literature, a few examples of halogen containing amino acids with a $sp^2$ C–Br bond can be found, mostly being derivatives of the natural aromatic amino acids phenylalanine [9], tryptophane [10], histidine [11] and tyrosine [12,13]. Another way to incorporate a reactive $sp^2$ C–Br bond into amino acids or peptides is the derivatization of the amino or carboxy group. Following this strategy, we synthesized a series of ten new bromo containing amino acid and peptide derivatives with the bromo substituent being part of a benzoyl moiety linked to the amino group (**1**–**6**; **a**, **b**, respectively; Fig. 1) in order to expand the pool of non-natural halogen containing amino acids and peptides as potential building blocks for bioconjugate formation. In view of this potential application, there is also interest in the knowledge of the solid state structures of the new compounds. Here we describe the preparation of the respective compounds (Fig. 1) and report the X-ray crystal struc-

*Abbreviations:* DMF, *N*,*N*-dimethylformamide; $Et_3N$, triethylamine; EtOAc, ethyl acetate; $Et_2O$, diethyl ether; MeOH, methanol; HOBt, 1-hydroxybenzotriazole; DCC, *N*,*N*′-dicyclohexylcarbodiimide; TMSCl, trimethylsilyl chloride; H–Gly–OMe, glycine methyl ester; H–Gly–Gly–OMe, glycylglycine methyl ester; DMSO, dimethyl sulfoxide.

* Corresponding author. Tel.: +49 3731 39 2386; fax: +49 3731 39 3170.
*E-mail address:* edwin.weber@chemie.tu-freiberg.de (E. Weber).

0022-2860/$ - see front matter © 2011 Elsevier B.V. All rights reserved.
doi:10.1016/j.molstruc.2011.03.058

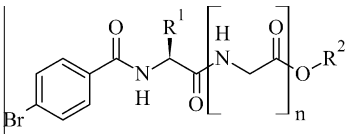

**1a** ($R^1$=$R^2$=H, n=0)
**1b** ($R^1$=Me, $R^2$=H, n=0)
**2** ($R^1$=$R^2$=H, n=1)
**3a** ($R^1$=H, $R^2$=Me, n=0)
**3b** ($R^1$=$R^2$=Me, n=0)
**4a** ($R^1$=H, $R^2$=Me, n=1)
**4b** ($R^1$=$R^2$=Me, n=1)
**5a** ($R^1$=H, $R^2$=Me, n=2)
**5b** ($R^1$=$R^2$=Me, n=2)
**6** ($R^1$=H, $R^2$=Me, n=3)

**Fig. 1.** Compound formulas of the *N*-(*p*-bromobenzoyl) substituted amino acid and peptide derivatives studied in this paper.

tures of the amino acid (**1a**, **1b**), the amino acid ester (**3a**, **3b**) and the peptide ester derivatives (**4a**, **4b**, **5b**).

## 2. Experimental

### 2.1. Materials and methods

Commercial chemicals (glycine, L-alanine, glycylglycine, *p*-bromobenzoic acid, TMSCl, 2,2-dimethoxypropane, HOBt·$H_2O$ and DCC) and solvents were used without further purification. Preparation of *p*-bromobenzoyl chloride, H–Gly–OMe·HCl and H–Gly–Gly–OMe·HCl was afforded using literature procedures [14,15].

Melting points (mp) were determined with a hot stage microscope and are uncorrected. Optical rotation measurements were performed on a Perkin–Elmer 241 polarimeter at 20 °C and with $\lambda$ = 589.3 nm ($Na_D$ line). $[\alpha]_D^{20}$ values are given in $10^{-1}$ $cm^2$ $g^{-1}$ (including the molar concentration and solvent used for the appropriate measurement). NMR spectra were recorded on a Bruker Avance III 500 NMR spectrometer at 500.13 MHz [$^1$H] and 125.76 MHz [$^{13}$C], respectively, at 25 °C and with DMSO-$d_6$ as solvent (unless otherwise stated). Chemical shifts ($\delta$) are given in ppm (referring to tetramethylsilane as internal standard) and coupling constants ($^3J_{HH}$, $^2J_{HH}$) in Hz. The multiplicity is given as s (singlet), d (doublet), dd (doublet of doublets), t (triplet), q (quintuplet), m (multiplet) or br s (broad singlet). IR spectra were measured on a Nicolet 510-FT-IR spectrometer (KBr pellets). Wave numbers ($\tilde{\nu}$) are given in $cm^{-1}$. IR spectroscopic data of all compounds are included in the Electronic supplementary material. MS spectra were obtained using a GC/MS system Hewlett–Packard 5890 Series II/MS 5989A (electron ionization). ESI-MS spectra were measured on a Varian 320-MS LC/MS system in positive (+) or negative (−) scan mode. Elemental analyses (EA) were performed on an Elementar Vario Micro Cube elemental analysator.

### 2.2. General procedure for the preparation of the substituted amino acid derivatives ***1a***, ***1b*** and of the corresponding dipeptide derivative ***2***

The amino acid or the peptide was dissolved in an aqueous solution of sodium hydroxide and finely powdered *p*-bromobenzoyl chloride was added portionwise under stirring. The reaction mixture was stirred for the appropriate reaction time and after separation of possibly remaining undissolved solid, the mixture was acidified dropwise with semi-concentrated hydrochloric acid under cooling in an ice bath. The resulting solid was separated, washed thoroughly with water and dried. Further details for each compound are specified below.

#### 2.2.1. *N*-(*p*-bromobenzoyl)glycine (***1a***)

NaOH (4.00 g, 100.0 mmol) in water (200 ml), glycine (3.75 g, 50.0 mmol) and *p*-bromobenzoyl chloride (10.97 g, 50.0 mmol) were used (reaction time: 3 h). The crude product was stirred in 100 ml of $Et_2O$, reseparated and dried to afford **1a** (10.39 g, 81 %), mp 163–164 °C [lit. [16]: 162 °C, lit. [17]: 163–164 °C (EtOH)]. $^1$H NMR: $\delta_H$ = 3.93 (2H, d, $^3J_{HH}$ = 5.85, C$H_2$); 7.71 (2H, d, $^3J_{HH}$ = 8.60, Ar–*H*); 7.82 (2H, d, $^3J_{HH}$ = 8.60, Ar–*H*); 8.95 (1H, d, $^3J_{HH}$ = 5.85, N*H*); 12.64 (1H, br s, CO–O*H*). $^{13}$C NMR: $\delta_C$ = 41.33 (*C*$H_2$); 125.29, 129.46, 131.51, 133.03 (Ar–*C*); 165.67 (*C*O–NH); 171.28 (*C*O–OH). ESI(−)-MS: *m/z* calcd for $C_9H_8BrNO_3$: 256.97, found: 255.6 $[M-H]^-$, 514.9 $[2M-H]^-$. EA: calcd: C, 41.89; H, 3.12; N, 5.43, found: C, 41.88; H, 3.26; N, 5.61.

#### 2.2.2. *N*-(*p*-bromobenzoyl)-L-alanine (***1b***)

NaOH (4.00 g, 100.0 mmol) in water (200 ml), L-alanine (4.45 g, 50.0 mmol) and *p*-bromobenzoyl chloride (10.97 g, 50.0 mmol) were used (reaction time: 7 h). The crude product was stirred in 125 ml of $Et_2O$, reseparated and dried. A second product fraction was obtained from the $Et_2O$ solution by concentrating it in vacuo and repetition of the purification process described before with 50 ml of $Et_2O$. A total yield of 11.07 g (81%) of **1b**, mp 155–158 °C, was afforded. $[\alpha]_D^{20}$ = + 9.3 (0.05 M, methanol). $^1$H NMR: $\delta_H$ = 1.41 (3H, d, $^3J_{HH}$ = 7.35, C$H_3$); 4.43 (1H, q, $^3J_{HH}$ = 7.25, C*H*); 7.70 (2H, d, $^3J_{HH}$ = 8.50, Ar–*H*); 7.86 (2H, d, $^3J_{HH}$ = 8.55, Ar–*H*); 8.79 (1H, d, $^3J_{HH}$ = 7.20, N*H*); 12.60 (1H, br s, CO–O*H*). $^{13}$C NMR: $\delta_C$ = 16.95 (*C*$H_3$); 48.36 (*C*H); 125.26, 129.69, 131.41, 133.12 (Ar–*C*); 165.35 (*C*O–NH); 174.23 (*C*O–OH). ESI(−)-MS: *m/z* calcd for $C_{10}H_{10}BrNO_3$: 270.98, found: 269.8 $[M-H]^-$, 542.9 $[2M-H]^-$. EA: calcd: C, 44.14, H, 3.70, N, 5.15, found: C, 44.08, H, 3.74, N, 4.88.

#### 2.2.3. *N*-(*p*-bromobenzoyl)glycylglycine (***2***)

NaOH (1.60 g, 40.0 mmol) in water (80 ml), glycylglycine (2.64 g, 20.0 mmol) and *p*-bromobenzoyl chloride (4.39 g, 20.0 mmol) were used (reaction time: 6.0 h). Further purification was afforded by recrystallization from ethanol to yield **2** (5.30 g, 84 %), mp 228–229 °C. $^1$H NMR: $\delta_H$ = 3.78, 3.91 (each 2H, each d, each $^3J_{HH}$ = 5.95, C$H_2$–CO–NH, C$H_2$–CO–OH); 7.70 (2H, d, $^3J_{HH}$ = 8.55, Ar–*H*); 7.83 (2H, d, $^3J_{HH}$ = 8.50, Ar–*H*); 8.24, 8.89 (each 1H, each t, each $^3J_{HH}$ = 5.95, N*H*); 12.58 (1H, br s, CO–O*H*). $^{13}$C NMR: $\delta_C$ = 40.69, 42.48 (*C*$H_2$–CO–NH, *C*$H_2$–CO–OH); 125.12, 129.56, 131.33, 133.22 (Ar–*C*); 165.62 (Ph–*C*O–NH); 169.24 (CH$_2$–*C*O–NH); 171.16 (*C*O–OH). ESI(+)-MS: *m/z* calcd for $C_{11}H_{11}BrN_2O_4$: 313.99, found: 336.9 $[M+Na]^+$, 653.0 $[2M+Na]^+$, 984.8 $[3M+K]^+$. EA: calcd: C, 41.93, H, 3.52, N, 8.89, found: C, 42.00, H, 3.67, N, 8.97.

### 2.3. General procedure for the preparation of the *N*-(*p*-bromobenzoyl) substituted amino acid ester derivatives ***3a*** and ***3b***

TMSCl (6.4 ml, 50.0 mmol) was added slowly to 25.0 mmol of the solid *N*-(*p*-bromobenzoyl) amino acid under an atmosphere of argon. 25 ml of dry MeOH were added to the resulting suspension in three portions and the mixture was stirred for 18 h at room temperature (argon atmosphere). The reaction mixture was concentrated in vacuo and the oily residue was dissolved in 50 ml of MeOH. Concentration of the MeOH solution under reduced pressure afforded a solid residue which was recrystallized from MeOH/$Et_2O$. Further details for each compound are specified below.

#### 2.3.1. *N*-(*p*-bromobenzoyl)glycine methyl ester (***3a***)

6.45 g (25.0 mmol) of **1a** were used to afford **3a** (6.37 g, 94%), mp 109–111 °C. $^1$H NMR ($CDCl_3$): $\delta_H$ = 3.80 (3H, s, C$H_3$); 4.22 (2H, d, $^3J_{HH}$ = 4.95, C$H_2$); 6.92 (1H, br s, N*H*); 7.56 (2H, d, $^3J_{HH}$ = 8.55, Ar–*H*); 7.68 (2H, d, $^3J_{HH}$ = 8.50, Ar–*H*). $^{13}$C NMR ($CDCl_3$):

$\delta_C$ = 41.70 ($CH_2$); 52.52 ($CH_3$); 126.56, 128.67, 131.82, 132.38 (Ar–*C*); 166.53 (*C*O–NH); 170.43 (*C*O–O–$CH_3$). MS: *m*/*z* calcd for $C_{10}H_{10}BrNO_3$: 270.98, found 271 $[M]^{+\cdot}$. EA: calcd: C, 44.14, H, 3.70, N, 5.15, found: C, 44.10, H, 3.71, N, 5.20.

*2.3.2. N-(p-bromobenzoyl)-L-alanine methyl ester (**3b**)*

6.80 g (25.0 mmol) of **1b** were used to yield **3b** (5.98 g, 84%), mp 96–98 °C. $[\alpha]_D^{20}$ = + 24.3 (0.05 M, acetone). $^1$H NMR: $\delta_H$ = 1.40 (3H, d, $^3J_{HH}$ = 7.35, CH–*CH*$_3$); 3.65 (3H, s, O–*CH*$_3$); 4.48 (1H, q, $^3J_{HH}$ = 7.25, *CH*); 7.71 (2H, d, $^3J_{HH}$ = 8.60, Ar–*H*); 7.84 (2H, d, $^3J_{HH}$ = 8.55, Ar–*H*); 8.91 (1H, d, $^3J_{HH}$ = 6.85, N*H*). $^{13}$C NMR: $\delta_C$ = 16.77 (CH–*CH*$_3$); 48.42 (*CH*); 52.01 (O–*CH*$_3$); 125.36, 129.67, 131.43, 132.81 (Ar–*C*); 165.40 (*C*O–NH); 173.13 (*C*O–O–$CH_3$). MS: *m*/*z* calcd for $C_{11}H_{12}BrNO_3$: 285.00, found: 285 $[M]^{+\cdot}$. EA: calcd: C, 46.18, H, 4.23, N, 4.90, found: C, 45.99, H, 4.29, N, 4.96.

*2.4. Synthesis of N-(p-bromobenzoyl)glycylglycine methyl ester (**4a**)*

To a suspension of **2** (4.73 g, 15.0 mmol) in 300 ml of 2,2-dimethoxypropane were added 15 ml of concentrated hydrochloric acid. The resulting mixture was stirred for 2 h at room temperature. After having left without stirring overnight, the mixture was concentrated cautiously in vacuo (max. bath temperature of 40 °C). The resulting solid was separated and washed with $Et_2O$. Further concentration of the reaction mixture and the combined $Et_2O$ solutions resulted in a second product fraction. Pure **4a** (3.15 g, 64%), mp 171–172 °C, was obtained by recrystallization from MeOH/$Et_2O$. $^1$H NMR: $\delta_H$ = 3.63 (3H, s, C*H*$_3$); 3.87 (2H, d, $^3J_{HH}$ = 5.90, C*H*$_2$); 3.92 (2H, d, $^3J_{HH}$ = 5.95, C*H*$_2$); 7.70 (2H, d, $^3J_{HH}$ = 8.55, Ar–*H*); 7.84 (2H, d, $^3J_{HH}$ = 8.55, Ar–*H*); 8.36 (1H, t, $^3J_{HH}$ = 5.85, N*H*); 8.89 (1H, t, $^3J_{HH}$ = 5.95, N*H*). $^{13}$C NMR: $\delta_C$ = 40.64, 42.46 (*CH*$_2$); 51.75 (*CH*$_3$); 125.17, 129.59, 131.35, 133.18 (Ar–*C*); 165.65 (Ph–*C*O–NH); 169.48, 170.31 (CH$_2$–*C*O–NH, *C*O–O–CH$_3$). ESI(+)-MS: *m*/*z* calcd for $C_{12}H_{13}BrN_2O_4$: 328.01, found: 328.9 $[M+H]^+$, 350.8 $[M+Na]^+$, 680.9 $[2M+Na]^+$. EA: calcd: C, 43.79, H, 3.98, N, 8.51, found: C, 43.59, H, 4.07, N, 8.66.

*2.5. General procedure for the preparation of the peptide ester derivatives **4b**, **5a**, **5b** and **6***

A mixture of H–Gly–OMe·HCl or H–Gly–Gly–OMe·HCl and dry DMF was neutralized with $Et_3N$. After stirring for 10 min, the *N*-(*p*-bromobenzoyl) amino acid or peptide was added and stirring was continued for another 10 min followed by the addition of HOBt·$H_2O$. After cooling to −10 °C, a solution of DCC in dry $CH_2Cl_2$ was added in small portions and the mixture was stirred for 2 h at −10 °C. After warming to room temperature, the suspension was stirred for 6 h and then left without stirring overnight. Further details for each compound are specified below.

*2.5.1. N-(p-bromobenzoyl)-L-alanylglycine methyl ester (**4b**)*

H–Gly–OMe·HCl (1.26 g, 10.0 mmol) in DMF (50 ml), $Et_3N$ (1.39 ml, 10.0 mmol), **1b** (2.72 g, 10.0 mmol), HOBt·$H_2O$ (1.68 g, 11.0 mmol) and DCC (2.27 g, 11.0 mmol) in $CH_2Cl_2$ (25 ml) were used. After separation of the solid, the filtrate was concentrated in vacuo and the resulting solid residue was added to 250 ml of EtOAc. After separation of insoluble material, the organic phase was washed twice with saturated $NaHCO_3$ solution (50 ml each), once with saturated NaCl solution (50 ml), dried over $Na_2SO_4$ and put into the refrigerator overnight. The solid which had crystallized (*N*,*N*′-dicyclohexyl urea) was separated and the solution concentrated to dryness in vacuo. The residue was recrystallized from MeOH/$Et_2O$ to afford **4b** (2.43 g, 71%), mp 135–137 °C. $[\alpha]_D^{20}$ = +24.6 (0.05 M, acetone). $^1$H NMR: $\delta_H$ = 1.35 (3H, d, $^3J_{HH}$ = 7.20, CH–*CH*$_3$); 3.63 (3H, s, O–*CH*$_3$); 3.82 (1H, dd, $^2J_{HH}$ = 17.35, $^3J_{HH}$ = 5.85, C*H*$_2$); 3.88 (1H, dd, $^2J_{HH}$ = 17.30, $^3J_{HH}$ = 5.95, C*H*$_2$); 4.52 (1H, q, $^3J_{HH}$ = 7.30, C*H*); 7.69 (2H, d, $^3J_{HH}$ = 8.45, Ar–*H*); 7.86 (2H, d, $^3J_{HH}$ = 8.45, Ar–*H*); 8.35 (1H, t, $^3J_{HH}$ = 5.85, CH$_2$–N*H*); 8.66 (1H, d, $^3J_{HH}$ = 7.50, CH–N*H*). $^{13}$C NMR: $\delta_C$ = 17.84 (CH–*CH*$_3$); 40.68 (*CH*$_2$); 48.85 (*CH*); 51.74 (O–*CH*$_3$); 125.11, 129.80, 131.24, 133.24 (Ar–*C*); 165.23 (Ph–*C*O–NH); 170.33, 172.91 (CH–*C*O–NH, *C*O–O–CH$_3$). ESI(+)-MS: *m*/*z* calcd for $C_{13}H_{15}BrN_2O_4$: 342.02, found: 364.9 $[M+Na]^+$, 380.9 $[M+K]^+$, 708.8 $[2M+Na]^+$. EA: calcd: C, 45.50, H, 4.41, N, 8.16, found: C, 45.59, H, 4.42, N, 8.35.

*2.5.2. N-(p-bromobenzoyl)glycylglycylglycine methyl ester (**5a**)*

H–Gly–OMe·HCl (1.26 g, 10.0 mmol) in DMF (50 ml), $Et_3N$ (1.39 ml, 10.0 mmol), **2** (3.15 g, 10.0 mmol), HOBt·$H_2O$ (1.68 g, 11.0 mmol) and DCC (2.27 g, 11.0 mmol) in $CH_2Cl_2$ (25 ml) were used. The solid was separated, stirred in 500 ml of boiling EtOAc, reseparated and dried on air. The purification step was repeated with 150 ml of boiling water to yield **5a** (2.96 g, 77%), mp 248–250 °C. $^1$H NMR: $\delta_H$ = 3.63 (3H, s, C*H*$_3$); 3.77 (2H, d, $^3J_{HH}$ = 5.75, C*H*$_2$); 3.87 (2H, d, $^3J_{HH}$ = 5.85, C*H*$_2$); 3.93 (2H, d, $^3J_{HH}$ = 5.70, C*H*$_2$); 7.71 (2H, d, $^3J_{HH}$ = 8.45, Ar–*H*); 7.84 (2H, d, $^3J_{HH}$ = 8.45, Ar–*H*); 8.27–8.30 (2H, m, 2×N*H*); 8.90 (1H, t, $^3J_{HH}$ = 5.70, N*H*). $^{13}$C NMR:

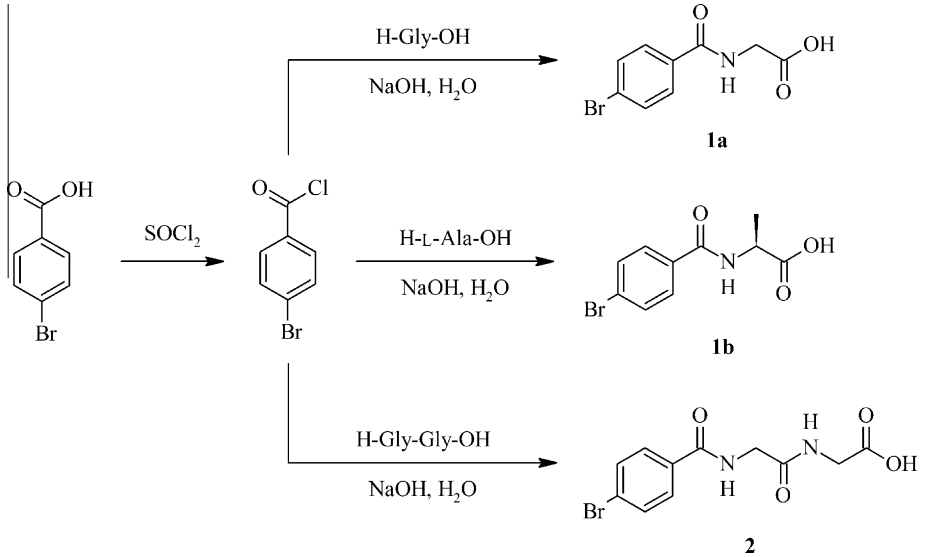


**Scheme 1.** Synthesis of compounds **1a**, **1b** and **2** starting from *p*-bromobenzoic acid.

$\delta_C$ = 40.53, 41.75, 42.74 ($CH_2$); 51.70 ($CH_3$); 125.13, 129.51, 131.30, 133.07 (Ar–*C*); 165.72 (Ph–*C*O–NH); 169.20, 169.38, 170.17 ($CH_2$–*C*O–NH, *C*O–O–$CH_3$). ESI(−)-MS: *m/z* calcd for $C_{14}H_{16}BrN_3O_5$: 385.03, found: 383.7 $[M-H]^-$. EA: calcd: C, 43.54, H, 4.18, N, 10.88, found: C, 43.53, H, 4.16, N, 10.86.

### 2.5.3. N-(p-bromobenzoyl)-L-alanylglycylglycine methyl ester (**5b**)

H–Gly–Gly–OMe·HCl (3.65 g, 10.0 mmol) in DMF (100 ml), $Et_3N$ (2.78 ml, 20.0 mmol), **1b** (5.44 g, 20.0 mmol), HOBt·$H_2O$ (3.37 g, 22.0 mmol) and DCC (4.54 g, 22.0 mmol) in $CH_2Cl_2$ (50 ml) were used. The reaction mixture was concentrated in vacuo, the residue stirred in 200 ml of boiling EtOAc, reseparated, stirred in 200 ml of boiling water, reseparated and dried on air. Pure **5b** (4.69 g, 59%), mp 194–196 °C, was afforded by recrystallization from MeOH/$Et_2O$. $[\alpha]_D^{20}$ = + 22.5 (0.05 M, methanol). $^1$H NMR: $\delta_H$ = 1.35 (3H, d, $^3J_{HH}$ = 7.15, CH–C$H_3$); 3.63 (3H, s, O–C$H_3$); 3.75 (2H, d, $^3J_{HH}$ = 5.90, C$H_2$); 3.88 (2H, d, $^3J_{HH}$ = 6.05, C$H_2$); 4.47 (1H, q, $^3J_{HH}$ = 7.10, C*H*); 7.69 (2H, d, $^3J_{HH}$ = 8.55, Ar–*H*); 7.86 (2H, d, $^3J_{HH}$ = 8.55, Ar–*H*); 8.23 (1H, t, $^3J_{HH}$ = 5.85, $CH_2$–N*H*); 8.28 (1H, t, $^3J_{HH}$ = 5.85, $CH_2$–N*H*); 8.71 (1H, d, $^3J_{HH}$ = 7.00, CH–N*H*). $^{13}$C NMR: $\delta_C$ = 17.64 (CH–$CH_3$); 40.63, 41.92 ($CH_2$); 49.35 (*C*H); 51.79 (O–$CH_3$); 125.20, 129.82, 131.27, 133.13 (Ar–*C*); 165.53 (Ph–*C*O–NH); 169.45, 170.25, 172.66 (CH–*C*O–NH, $CH_2$–*C*O–NH, *C*O–O–$CH_3$). ESI(+)-MS: *m/z* calcd for $C_{15}H_{18}BrN_3O_5$: 399.04, found: 399.9 $[M+H]^+$, 423.8 $[M+Na]^+$, 822.9 $[2M+Na]^+$. EA: calcd: C, 45.01, H, 4.53, N, 10.50, found: C, 45.11, H, 4.62, N, 10.48.

### 2.5.4. N-(p-bromobenzoyl)glycylglycylglycylglycine methyl ester (**6**)

H–Gly–Gly–OMe·HCl (0.37 g, 2.0 mmol) in DMF (10.0 ml), $Et_3N$ (0.28 ml, 2.0 mmol), **2** (0.63 g, 2.0 mmol), HOBt·$H_2O$ (0.34 g,

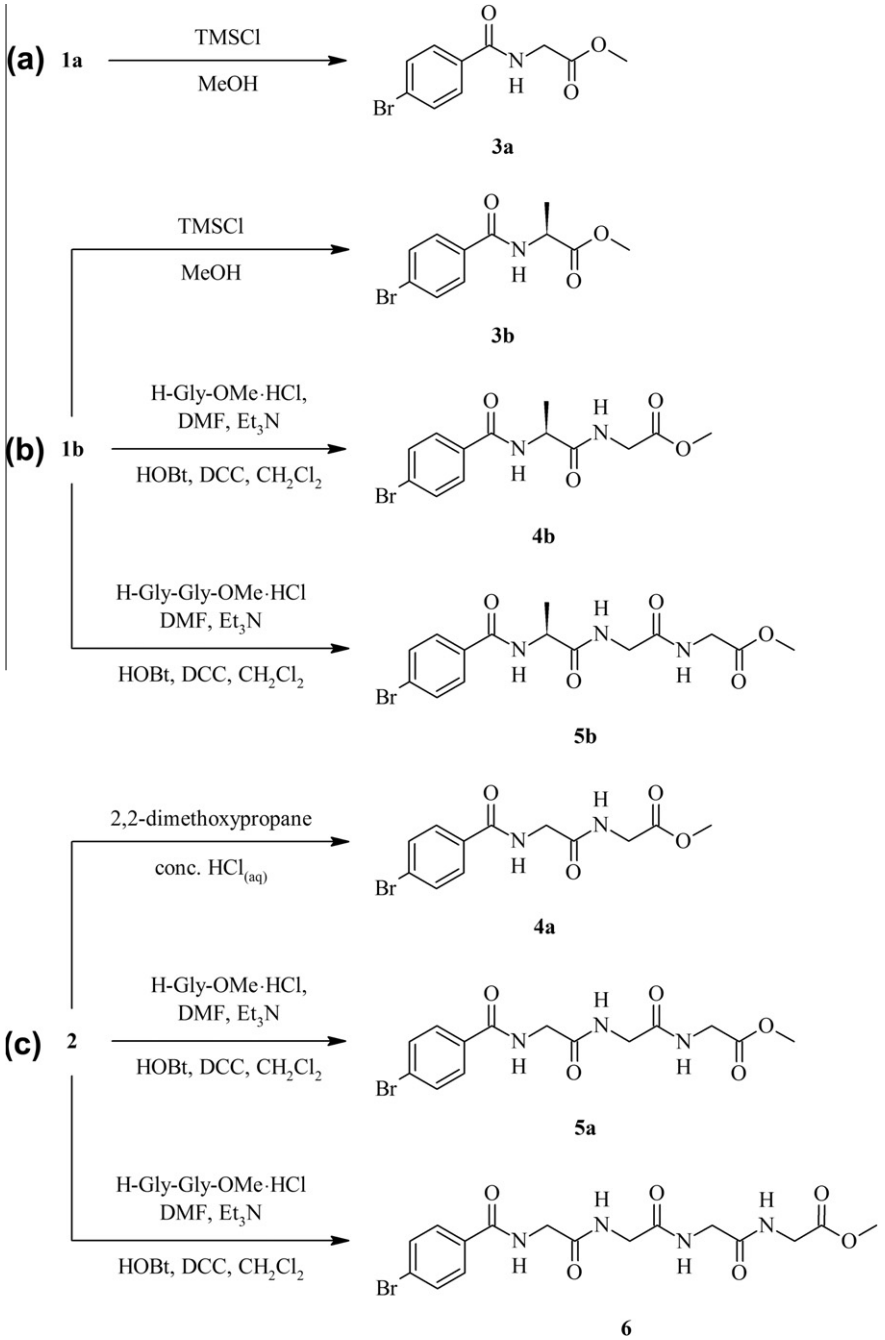


**Scheme 2.** Synthesis of *N*-(*p*-bromobenzoyl) substituted amino acid and peptide ester derivatives **3a**, **3b**, **4a**, **4b**, **5a**, **5b** and **6**.

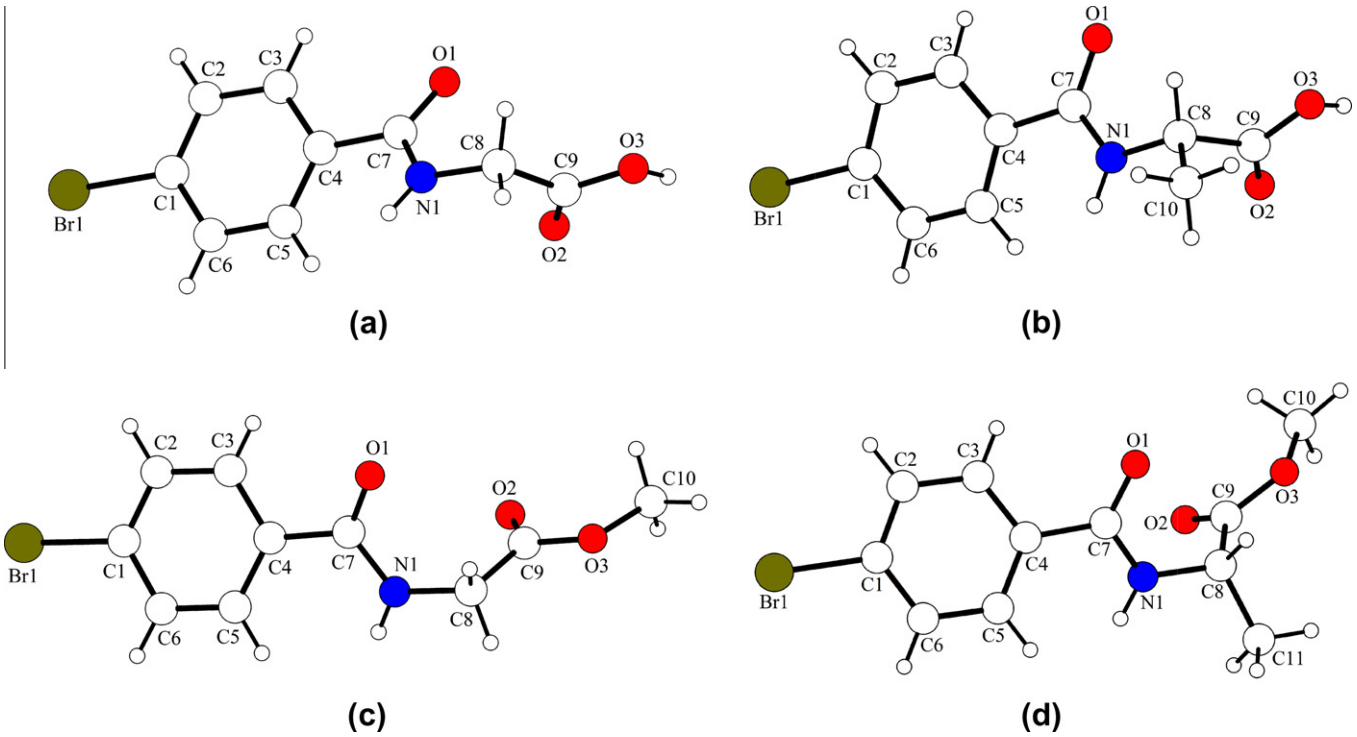


**Fig. 2.** Molecular structures of compounds **1a** (a), **1b** (b), **3a** (c) and **3b** (d) including atom numbering schemes.

**Table 1**
Selected torsion angles (°) for compounds **1a**, **1b**, **3a** and **3b**.

| Torsion angle | 1a | 1b | 3a | 3b |
|---|---|---|---|---|
| C3–C4–C7–O1 | −28.9(5) | −18.8(3) | 21.3(4) | 29.6(2) |
| C4–C7–N1–C8($\omega_{-1*}$) | 178.7(3) | −175.23(15) | −179.2(2) | 178.51(12) |
| C7–N1–C8–C9 ($\varphi_1$) | −67.3(4) | −88.7(2) | −76.9(3) | −78.89(16) |
| C7–N1–C8–C10/C11[a] | – | 147.81(17) | – | 160.14(13) |
| C8–C9–O3–C10 ($\omega_{1*}$) | – | – | 173.4(2) | 176.52(13) |
| N1–C8–C9–O3 ($\psi_{1*}$) | 170.4(3) | 160.24(15) | 174.6(2) | 143.25(12) |
| O1–C7–N1–C8 | −0.1(5) | 3.5(3) | −1.1(4) | −1.5(2) |

[a] The relevant atoms are C10 for **1b** and C11 for **3b**, respectively.

2.2 mmol) and DCC (0.45 g, 2.2 mmol) in $CH_2Cl_2$ (5.0 ml) were used. The solid was separated, stirred in 100 ml of boiling EtOAc, reseparated and dried on air to yield **6** (0.60 g, 68%), mp 268–270 °C. $^1$H NMR: $\delta_H$ = 3.62 (3H, s, $CH_3$); 3.76–3.78 (4H, m, 2×$CH_2$); 3.84 (2H, d, $^3J_{HH}$ = 5.80, $CH_2$); 3.93 (2H, d, $^3J_{HH}$ = 5.65, $CH_2$); 7.70 (2H, d, $^3J_{HH}$ = 8.35, Ar–*H*); 7.83 (2H, d, $^3J_{HH}$ = 8.40, Ar–*H*); 8.19 (1H, t, $^3J_{HH}$ = 5.70, N*H*); 8.23–8.28 (2H, m, 2×N*H*); 8.91 (1H, t, $^3J_{HH}$ = 5.55, N*H*). $^{13}$C NMR: $\delta_C$ = 40.62, 41.81, 42.20, 42.86 ($CH_2$); 51.81 ($CH_3$); 125.26, 129.63, 131.42, 133.17 (Ar–*C*); 165.87 (Ph–*C*O–NH); 169.28, 169.43, 169.44, 170.28 ($CH_2$–*C*O–NH, *C*O–O–$CH_3$). ESI(−)-MS: *m*/*z* calcd for $C_{16}H_{19}BrN_4O_6$: 442.05, found: 479.0 [M+Cl]$^-$. EA: calcd: C, 43.36, H, 4.32, N, 12.64, found: C, 43.09, H, 4.22, N, 12.60.

### 2.6. X-ray crystal structure analyses

The X-ray crystal structure analyses were performed using a Bruker Kappa diffractometer equipped with an Apex II CCD area detector and graphite-monochromatized Mo Kα radiation ($\lambda$ = 0.71073 Å) employing $\varphi$ and $\omega$ scan modes. The data were corrected for Lorentz and polarization effects. Semi-empirical absorption corrections were applied using the SADABS program and the SAINT program was utilized for integration of the diffraction

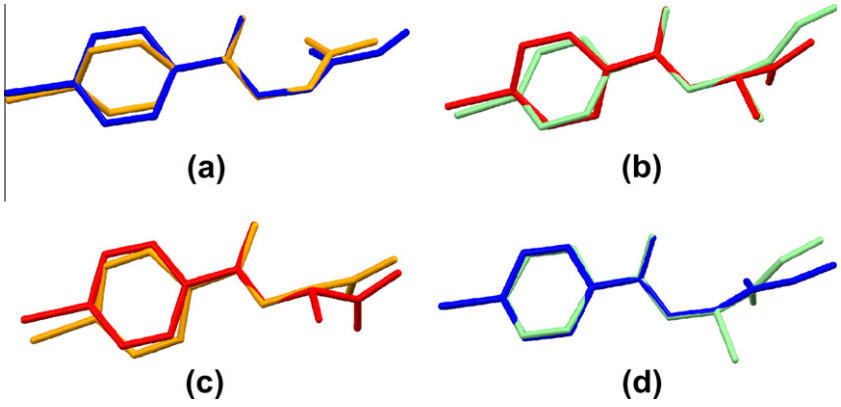


**Fig. 3.** Structure overlays for (a) **1a** (orange)/**3a** (blue) [RMS = 0.00874], (b) **1b** (red)/**3b** (green) [RMS = 0.0198], (c) **1a** (orange)/**1b** (red) [RMS = 0.0289] and (d) **3a** (blue)/**3b** (green) [RMS = 0.0130], calculated from the atoms O1, C7, N1 and C8, respectively. H atoms are omitted for clarity. (For interpretation of the references to color in this figure legend, the reader is referred to the web version of this article.)

**Table 2**
Hydrogen bonds in the crystal structures of compounds **1a**, **1b**, **3a** and **3b**.

| Atoms involved | Symmetry | Distance (Å) | | Angle (°) |
|---|---|---|---|---|
| | | *D*(D···A) | *d*(H···A) | *θ*(D–H···A) |
| ***1a*** | | | | |
| N1–H1···O1 | $x+1, y, z$ | 2.854(4) | 2.11 | 142.2 |
| O3–H3A···O2 | $-x, -y+1, -z+2$ | 2.673(4) | 1.84 | 175.0 |
| C6–H6···O1 | $x+1, y+1, z$ | 3.304(5) | 2.51 | 141.8 |
| ***1b*** | | | | |
| N1–H1···O2 | $-x+2, -x+y+1, -z+5/3$ | 2.9452(19) | 2.08 | 166.8 |
| O3–H3A···O1 | $x-y+1, -y+2, -z+4/3$ | 2.6210(19) | 1.88(2) | 165(2) |
| C5–H5···O2 | $-x+2, -x+y+1, -z+5/3$ | 3.338(2) | 2.49 | 148.6 |
| ***3a*** | | | | |
| N1–H1···O1 | $x-1/2, y, -z+3/2$ | 2.811(3) | 1.97 | 159.8 |
| C5–H5···O1 | $x-1/2, y, -z+3/2$ | 3.240(3) | 2.54 | 130.5 |
| C5–H5···O2 | $-x, y+1/2, -z+3/2$ | 3.206(4) | 2.49 | 132.3 |
| C8–H8A···*Cg*[a] | $-x, y+1/2, -z+3/2$ | 3.586(3) | 2.62 | 164.0 |
| C8–H8B···O2 | $-x+1/2, y+1/2, z$ | 3.555(4) | 2.59 | 165.1 |
| ***3b*** | | | | |
| N1–H1···O1 | $x+1, y, z$ | 2.9810(16) | 2.13 | 162.7 |
| C10–H10B···O2 | $-x+1, y+1/2, -z+3/2$ | 3.455(2) | 2.55 | 153.1 |
| C11–H11C···O3 | $x+1, y, z$ | 3.4942(19) | 2.60 | 151.2 |

[a] *Cg* is the centroid of the aromatic ring.

profiles [18]. The crystal structures were solved by direct methods using SHELXS-97 and refined by full-matrix least-squares refinement against $F^2$ using SHELXL-97 [19]. All non-hydrogen atoms were refined anisotropically; hydrogen atoms were generated at ideal geometrical positions and refined with the appropriate riding model or positioned by Difference Fourier synthesis. Geometrical calculations were performed using PLATON [20] and molecular graphics were generated using SHELXTL [19].

## 3. Results and discussion

### 3.1. Synthesis

The first step in the preparation of the discussed compounds was the introduction of the *p*-bromobenzoyl group into the amino acids glycine and L-alanine and into the peptide glycylglycine (Scheme 1). For this purpose, *p*-bromobenzoic acid was converted to the corresponding *p*-bromobenzoyl chloride [14], which was then reacted with glycine, L-alanine and glycylglycine under Schotten–Baumann conditions, respectively, to afford the *N*-(*p*-bromobenzoylated) derivatives **1a**, **1b** and **2**.

Starting from compound **1a** (Scheme 2a), the corresponding glycine methyl ester **3a** was obtained by esterification with TMSCl/MeOH using the protocol described by Li and Sha [15]. Analogously, compound **1b** (Scheme 2b) was converted to the appropriate ester derivative **3b**.

Peptide coupling of the L-alanine derivative **1b** with H–Gly–OMe·HCl using HOBt/DCC [21] (according to literature procedures [22,23]) afforded the *N*-(*p*-bromobenzoyl)-L-alanylglycine derivative **4b**. The corresponding L-alanine derived tripeptide **5b** could

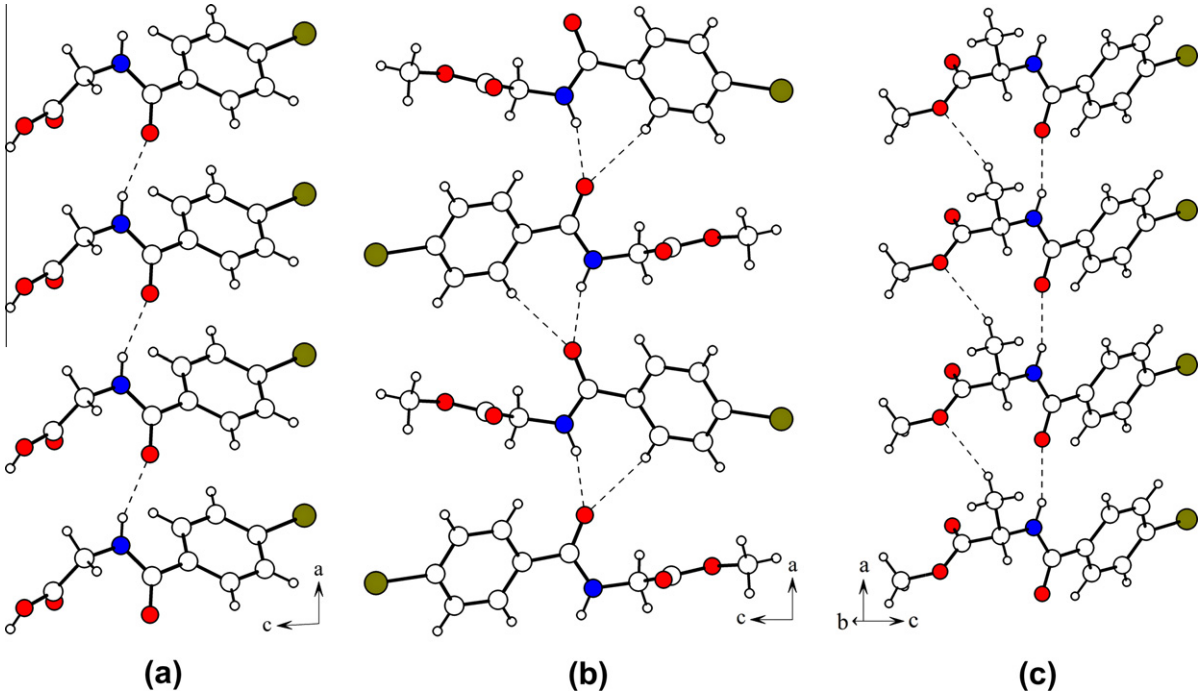


**Fig. 4.** Strand formation within the crystal structures of **1a** (a), **3a** (b) and **3b** (c). Hydrogen bonding interactions are represented as dashed lines.

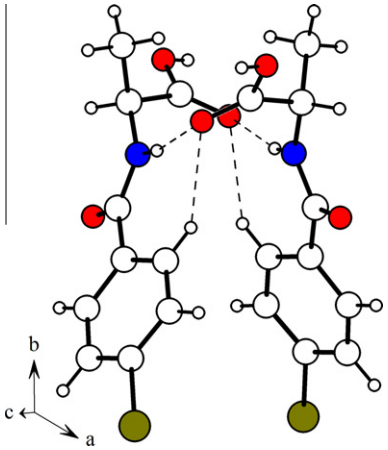


**Fig. 5.** Formation of molecule pairs in the crystal structure of compound **1b**. Hydrogen bonding interactions are represented as dashed lines. The first level graph set notations [25] for the N1–H1···O2 and the C5–H5···O2 interactions stabilizing the structural motif are $R_2^2(10)$ and $R_2^2(16)$, respectively.

be obtained accordingly using H–Gly–Gly–OMe·HCl for the peptide coupling step (Scheme 2b).

The dipeptide methyl ester **4a** resulted from esterification of compound **2** (Scheme 2c) with 2,2-dimethoxypropane/conc. $HCl_{(aq)}$ following a literature protocol [24]. Compound **2** could also be converted to the *N*-(*p*-bromobenzoyl)glycylglycylglycine derivative **5a** and the corresponding tetrapeptide derivative **6** by HOBt/DCC mediated peptide coupling with H–Gly–OMe·HCl and H–Gly–Gly–OMe·HCl, respectively.

### 3.2. Crystallization

Crystals suitable for X-ray crystal structure determination were obtained by slow evaporation of solutions of the respective compounds in solvents as specified in the following: **1a** (DMSO), **1b** (MeOH), **3a** ($Et_2O$), **3b** (MeOH/$Et_2O$), **4a** (MeOH/$Et_2O$), **4b** (MeOH), **5b** (MeOH). The crystallographic data and refinement details of all compounds studied are summarized in Table SUP-1.

### 3.3. Crystal structures of the amino acid derivatives *1a*, *1b*, *3a* and *3b*

At a first glance, the molecular structures of the amino acid derivatives **1a**, **1b**, **3a** and **3b** (Fig. 2) do not seem to differ significantly from each other. However, a detailed view of selected torsions angles (Table 1) reveals some obvious differences. As expected, in all molecules the amide bond is nearly planar and *trans* configurated, which can be derived from the torsion angles O1–C7–N1–C8 [values ranging from −1.5(2) to 3.5(3)°] and $\omega_{-1*}$ [absolute values ranging from 175.23(15) to 179.2(2)°], respectively. Differences occur in the torsion of the phenyl ring with reference to the amide bond, where torsion angles C3–C4–C7–O1 from −28.9(5) to 29.6(2)° are found. The torsion of the carboxylic C atom C9 in relation to the planar amide fragment is also different for the discussed amino acid derivatives [−67.3(4) to −88.7(2)° for $\varphi_1$]. Moreover, the difference in the torsion angle $\varphi_1$ consequently leads to a different torsion angle of the methyl group in the L-alanine derivatives **1b** and **3b** [147.81(17) and 160.14(13)° for C7–N1–C8–C10/C11, respectively]. Structural overlay plots (based on the atoms O1, C7, N1 and C8 of the rigid amide bond), making these structural differences more obvious, are given in Fig. 3.

The packing structures of **1a**, **1b**, **3a** and **3b** are characterized by numerous hydrogen bonding interactions. In particular, the amide N–H group plays an important part as hydrogen bonding donor site. Thus, in all structures, N–H···O contacts contribute to the formation of structural motifs. In the packing arrangements of **1a**, **3a** and **3b**, N1–H1···O1 contacts (Table 2) of $C_1^1(4)$ unitary level graph set [25] lead to the formation of strands running along the crystallographic *a* axis (Fig. 4). Regarding these strands, an alternating sequence of molecular orientations is found for compound **3a**, while

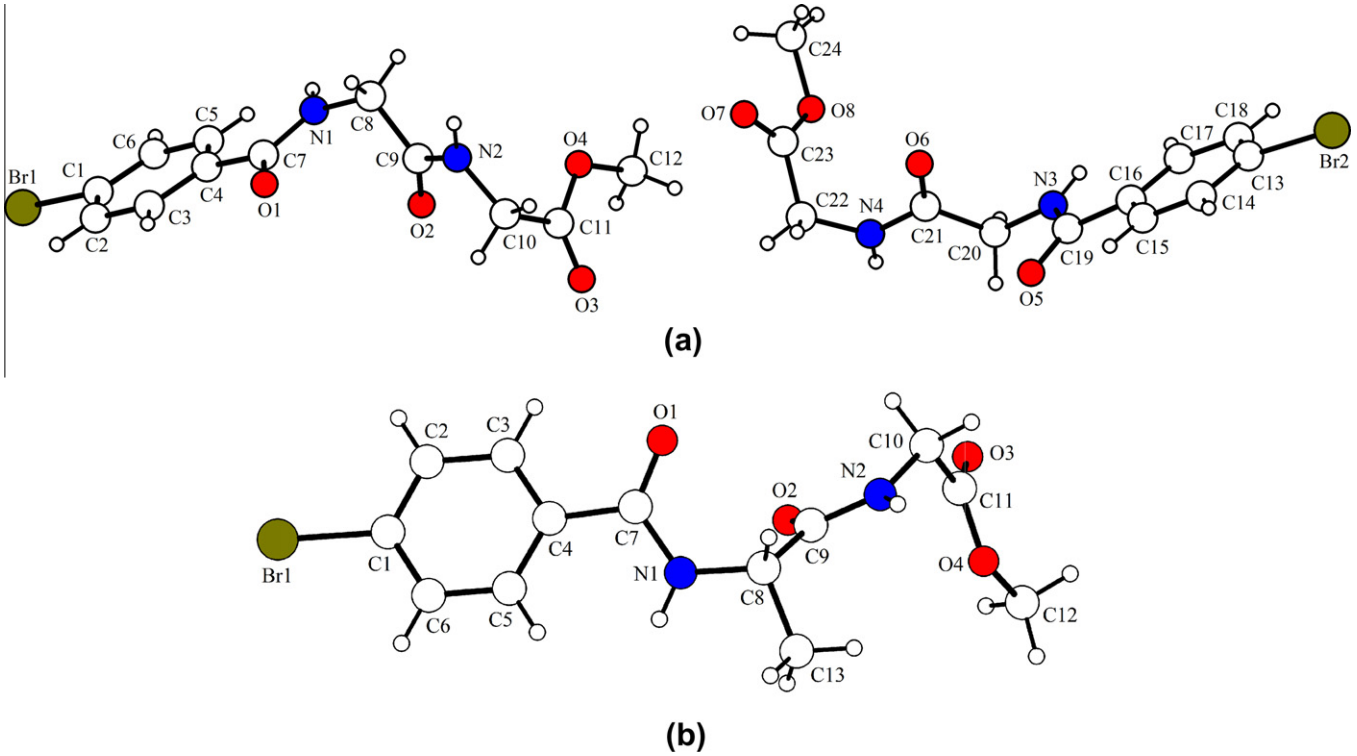


**Fig. 6.** Asymmetric units of the crystal structures of compounds **4a** (a) and **4b** (b) including atom numbering schemes.

**Table 3**
Selected torsion angles (°) for compounds **4a** and **4b**.

| Torsion angle | **4a** | | **4b** |
|---|---|---|---|
| | **4a**′ | **4a**″ | |
| C3–C4–C7–O1/C15–C16–C19–O5[a] | 7.9(4) | −8.9(5) | 24.6(2) |
| C4–C7–N1–C8/C16–C19–N3–C20[a] ($\omega_{-1*}$) | −179.8(3) | 176.7(3) | −178.32(13) |
| C7–N1–C8–C9/C19–N3–C20–C21[a] ($\varphi_1$) | 68.5(4) | 74.1(4) | −67.79(18) |
| C7–N1–C8–C13 | – | – | 170.48(14) |
| C8–C9–N2–C10/C20–C21–N4–C22[a] ($\omega_1$) | −178.4(3) | 175.7(3) | −173.69(13) |
| C9–N2–C10–C11/C21–N4–C22–C23[a] ($\varphi_2$) | 59.6(4) | 61.5(4) | −66.2(2) |
| C10–C11–O4–C12/C22–C23–O8–C24[a]($\omega_{2*}$) | 178.5(3) | 177.4(3) | −174.82(18) |
| N1–C8–C9–N2/N3–C20–C21–N4[a] ($\psi_1$) | −159.7(3) | −176.5(3) | 158.65(13) |
| N2–C10–C11–O4/N4–C22–C23–O8[a] ($\psi_{2*}$) | 34.6(4) | 33.5(4) | −38.1(2) |
| O1–C7–N1–C8/O5–C19–N3–C20[a] | 0.4(5) | −1.3(4) | 0.7(2) |
| O2–C9–N2–C10/O6–C21–N4–C22[a] | −1.0(5) | −4.9(5) | 7.3(2) |

[a] The first torsion angle refers to **4a**′ and **4b**, the second to **4a**″, respectively.

**Table 4**
Hydrogen bonds in the crystal structures of compounds **4a** and **4b**.

| Atoms involved | Symmetry | Distance (Å) | | Angle (°) |
|---|---|---|---|---|
| | | $D$(D···A) | $d$(H···A) | $\theta$(D–H···A) |
| ***4a*** | | | | |
| N1–H1N···O1 | $x, -y+1, z+1/2$ | 2.846(3) | 2.02 | 155.8 |
| N2–H2N···O2 | $x+1, y, z$ | 2.851(4) | 2.00 | 161.7 |
| N3–H3N···O5 | $x, -y+2, z+1/2$ | 2.841(3) | 2.02 | 154.6 |
| N4–H4N···O6 | $x-1, y, z$ | 2.854(3) | 2.01 | 160.1 |
| C5–H5···O1 | $x, -y+1, z+1/2$ | 3.477(4) | 2.57 | 159.6 |
| C8–H8A···O2 | $x+1, y, z$ | 3.163(4) | 2.48 | 125.6 |
| C10–H10B···O3 | $x+1, y, z$ | 3.201(4) | 2.39 | 138.9 |
| C12–H12B···Br1 | $x+1, -y+1, z+1/2$ | 3.802(4) | 2.84 | 166.5 |
| C12–H12B···O7 | $x, y, z$ | 3.022(4) | 2.44 | 117.4 |
| C17–H17···O5 | $x, -y+2, z+1/2$ | 3.470(4) | 2.55 | 162.5 |
| C22–H22B···O7 | $x-1, y, z$ | 3.208(4) | 2.38 | 141.1 |
| ***4b*** | | | | |
| N1–H1N···O1 | $x, y, z+1$ | 3.2490(17) | 2.39 | 165.1 |
| N2–H2N···O2 | $x+1, y, z$ | 2.8370(16) | 1.99 | 161.6 |
| C8–H8···O2 | $x+1, y, z$ | 3.1889(18) | 2.54 | 122.6 |
| C10–H10A···O3 | $x+1, y, z$ | 3.310(2) | 2.48 | 141.3 |
| C13–H13A···O1 | $x+1, y, z+1$ | 3.520(2) | 2.58 | 161.2 |

in **1a** and **3b** a regular, non-alternating arrangement is formed. Unlike in **1a**, the strands of **3a** are additionally stabilized by a weak (aryl)C5–H5···O1 interaction [26] of $C_1^1(5)$ synthon mode [25], leading to the formation of a bifurcated-acceptor type hydrogen bond [27] (Fig. 4b), while in the strands of **3b** a C–H···O contact (C11–H11C···O3, $C_1^1(5)$ motif [25]) contributes to a further stabilization (Fig. 4c). Within the packing of **1b**, the N–H···O interaction does not lead to a strand motif but to the formation of molecular pairs (Fig. 5), assisted by a weak (aryl)C–H···O contact (C5–H5···O2). Besides the discussed N–H···O interactions, O–H···O contacts comprising the carboxylic acid function participate in the formation of the crystal structures of compounds **1a** and **1b**. In **1a** a classical carboxylic acid dimer [28] of $R_2^2(8)$ synthon mode [29] is found, while in **1b** the carbonyl O2 atom is, among others, the acceptor for the N–H···O contact and the hydroxy O–H function acts as a donor for an O3–H3A···O1 interaction connecting the molecule pairs in *c* direction.

The interactions between different strands or molecular pairs within the packing structures are mainly of a weaker nature. In **1a**, the strands are side-connected via the carboxylic acid dimerization interaction mentioned above on one edge and a Br···Br interaction of the so-called 'side on' mode [30,31] ($D$(Br1···Br1$^i$) = 3.5952(5) Å, $\theta$(C1–Br1···Br1$^i$) = 98.08(11)°, $\theta$(C1$^i$–Br1$^i$···Br1) = 171.24(11)°, symmetry code $i = -x+3/2, y-1/2, -z+3/2$) on the other edge. In the structures of **1a**, **3a** and **3b**, additional weaker C–H···O contacts comprising aromatic, methylene and methyl C atoms as hydrogen bonding donors can be found (Table 2).

### 3.4. Crystal structures of the dipeptide derivatives *4a* and *4b*

The asymmetric units of the dipeptide crystal structures **4a** and **4b** are represented in Fig. 6. It is remarkable that the asymmetric unit of compound **4a** consists of two independent dipeptide molecules (**4a**′ on the left and **4a**″ on the right side of Fig. 6a). However, a comparison of the relevant torsion angles of **4a**′ and **4a**″ (Table 3) does not show any significant differences between one and another which is also obvious from the molecular overlay plot in Fig. 7a. In contrast to the molecular structure of **4a**, in **4b** the aromatic ring is distorted to a greater extent towards the neighboring amide bond [torsion angles C3–C4–C7–O1 = 7.9(4)° for **4a**′ and C15–C16–C19–O5 = −8.9(5)° for **4a**″ as well as C3–C4–C7–O1 = 24.6(2)° for **4b**]. These particular differences in the distortion of the aromatic ring are visualized in Fig. 7b and Fig. 7c. Similar to the amino acid derivatives (**1a**, **1b**, **3a**, **3b**), the amide bonds of the dipeptide derivatives are also approximately planar and *trans* configurated (cf. respective torsion angles in Table 3). Fig. 7b and Fig. 7c also clearly show that **4a** and **4b** differ in the conformation of the peptide chain. Thus, different values for the torsion angle $\varphi_1$ are found [68.5(4)°/74.1(4)° for **4a**′/**4a**″ and −67.79(18)° for **4b**, respectively]. Further differences in the peptide chains of the two dipeptide derivatives **4a** and **4b** are found for the torsion angles $\psi_1$, $\varphi_2$ as well as $\psi_{2*}$ (Table 3).

Just as discussed for the amino acid derivatives (**1a**, **1b**, **3a**, **3b**), the packing structures of compounds **4a** and **4b** are predominantly characterized by $C_1^1(4)$ type [25] N–H···O contacts between the amide N–H groups as donors and carbonyl O atoms as acceptors (excluding the C terminal amide carbonyl group in the case of the dipeptide derivatives **4a** and **4b**; Table 4). In the crystal structures both the N1–H1N···O1 (for **4a**″ N3–H3N···O5) and the N2–H2N···O2 (for **4a**″ N4–H4N···O6) interactions lead to the formation of strand structures with the strands running parallel along the *c* and *a* axis, respectively. On closer examination of the strands parallel to the *c* axis, these strands in the packing arrangement of

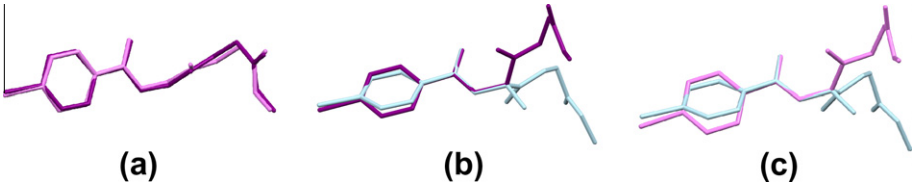


**Fig. 7.** (a) Structure overlay of the components of the asymmetric unit of compound **4a** [**4a**′ (purple)/**4a**″ (violet) with RMS = 0.2636] calculated from all non H atoms as well as structure overlays for (b) **4a**′ (purple)/**4b** (light blue) [RMS = 0.0151] and (c) **4a**″ (violet)/**4b** (light blue) [RMS = 0.0146], calculated from the atoms O1, C7, N1 and C8, respectively. H atoms are omitted for clarity. (For interpretation of the references to color in this figure legend, the reader is referred to the web version of this article.)

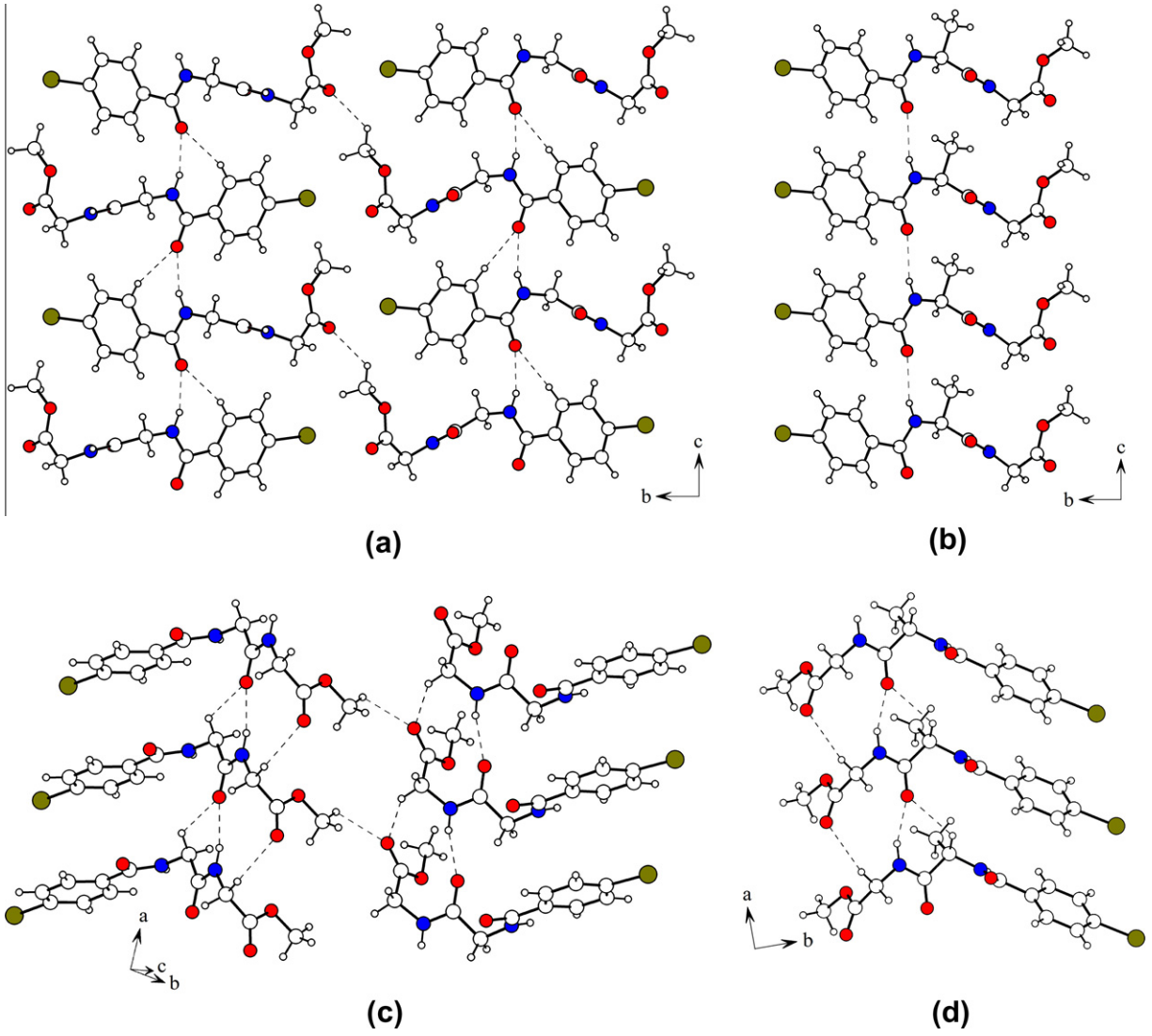


**Fig. 8.** Strand formation within the crystal structures of compounds **4a** and **4b** with strands running parallel to the *c* axis [**4a** (a), **4b** (b)] and *a* axis [**4a** (c), **4b** (d)], respectively. Hydrogen bonding interactions are represented as dashed lines.

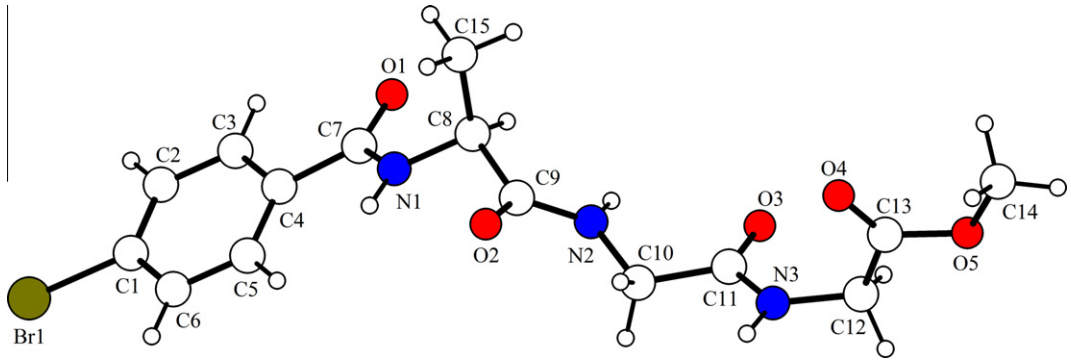


**Fig. 9.** Molecular structure of compound **5b** including the atom numbering scheme.

compound **4a** consist of alternately arranged dipeptide molecules where the strand formation is assisted by an (aryl)C–H···O contact (C5–H5···O1 and C17–H17···O5, respectively, $C_1^1(5)$ synthon mode [25]) leading to a bifurcated-acceptor type hydrogen bonding motif (cf. compound **3a**; Fig. 8a). In the case of compound **4b**, the N1–H1N···O1 interaction is of a weaker nature [$D$(D···A) = 3.2490(17) Å, $d$(H···A) = 2.39 Å] compared to the other N–H···O contacts discussed so far. Nevertheless, this contact contributes to the formation of strands parallel to the *c* axis with a non-alternating molecule orientation (Fig. 8b). In both crystal structures, the molecules within the strands running parallel to the *a* axis are predominantly linked via N2–H2N···O2 (for **4a**″ N4–H4N···O6)

**Table 5**
Hydrogen bonding interactions in the crystal structure of compound **5b**.

| Atoms involved | Symmetry | Distance (Å) | | Angle (°) |
|---|---|---|---|---|
| | | $D$(D···A) | $d$(H···A) | $\theta$(D–H···A) |
| N1–H1N···O3 | $-x+1, y-1/2, -z+3/2$ | 3.020(4) | 2.22 | 150.1 |
| N2–H2N···O2 | $-x+1, y+1/2, -z+3/2$ | 2.880(4) | 2.04 | 158.7 |
| N3–H3N···O1 | $-x+1, y-1/2, -z+3/2$ | 2.901(4) | 2.07 | 156.2 |
| C3–H3···O4 | $-x+3/2, -y+2, z+1/2$ | 3.280(5) | 2.46 | 143.8 |
| C5–H5···O3 | $-x+1, y-1/2, -z+3/2$ | 3.155(4) | 2.49 | 127.3 |
| C10–H10B···O1 | $-x+1, y-1/2, -z+3/2$ | 3.144(4) | 2.38 | 133.7 |
| C12–H12B···O4 | $x-1/2, -y+3/2, -z+1$ | 3.271(5) | 2.46 | 138.3 |
| C14–H14B···O2 | $x-1/2, -y+3/2, -z+1$ | 3.313(5) | 2.60 | 129.3 |

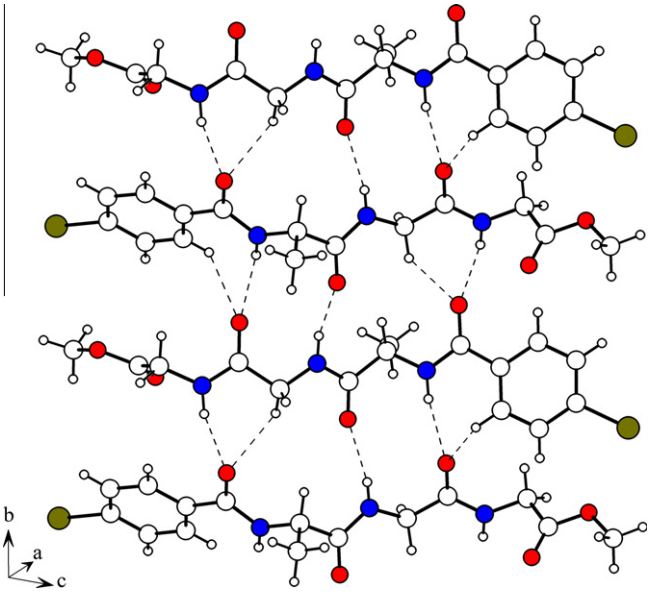


**Fig. 10.** Sheet formation within the crystal structure of compound **5b**. Hydrogen bonding interactions are represented as dashed lines.

hydrogen bonding interactions (Fig. 8c and d). Additional contributions to the strand formation emanate from numerous weak C–H···O interactions (**4a′**: C8–H8A···O2, C10–H10B···O3; **4a″**: C22–H22B···O7, **4b**: C8–H8···O2, C10–H10A···O3; $C_1^1(4)$ first level graph set [25], respectively; Table 4). Besides the hydrogen bonding interactions mentioned so far, additional intermolecular contacts stabilizing the packing structures are listed in Table 4. As these interactions are of the (alkyl)C–H···O [26] and (alkyl)C–H···Br contact mode [32], they can be considered as interactions of rather weak nature.

### 3.5. Crystal structure of the tripeptide derivative *5b*

The molecular structure of the tripeptide **5b** is illustrated in Fig. 9. Relevant torsion angles are given in Table SUP-2. As mentioned for the compounds above, the three amide bonds of **5b** are again nearly planar and *trans* configurated (cf. appropriate torsion angles in Table SUP-2).

In the packing of compound **5b**, the most dominant interactions are N–H···O contacts (N1–H1N···O3, N2–H2N···O2, N3–H3N···O1, Table 5) leading to the formation of sheet structures with an alternating molecule orientation (Fig. 10), similar to the antiparallel β-sheet motif known as a typical peptide secondary structure [33]. Considering unitary level graph sets [25], the N1–H1N···O3, N2–H2N···O2 and N3–H3N···O1 contacts can be described using the notations $C_1^1(8)$, $C_1^1(4)$ and $C_1^1(10)$, respectively, reflecting the antiparallel molecule orientation within the sheets. Besides the three N–H···O type interactions, weaker C–H···O contacts [26] (C5–H5···O3, C10–H10B···O1) participate in the formation of the sheets elongated parallel to the *b* axis. In the crystal structure of **5b**, different sheets are linked via additional C–H···O interactions (C3–H3···O4, C12–H12B···O4, C14–H14B···O2).

## 4. Conclusions

A series of new non-natural amino acid and peptide derivatives featuring *N*-(*p*-bromobenzoyl) substituents has been synthesized and characterized successfully. The discussed compounds seem promising as useful building blocks for the construction of different bioconjugates. The synthetic strategy is based on rather simple starting materials being commercially available, such as *p*-bromobenzoic acid, glycine, L-alanine or glycylglycine. Standard coupling methods and characteristic protecting and activating techniques were used for the formation of amide or peptide bonds. Thus, a way for the synthesis of similar amino acid or peptide derivatives using analogous starting materials for the coupling steps has been made accessible.

X-ray crystal structures obtained from compounds **1a**, **1b**, **3a** and **3b**, being amino acid or amino acid ester derivatives, as well as from the peptide ester derivatives **4a**, **4b** and **5b**, all show molecular structures with amide or peptide bonds being planar and *trans* configurated. The *p*-bromobenzoyl moiety is found slightly distorted with reference to the neighboring amide bond. In the crystals, N–H···O contacts can be considered as dominating intramolecular interactions contributing to the formation of characteristic structural motifs of the packing arrangements, namely strands (**1a**, **3a**, **3b**, **4a**, **4b**), molecular pairs (**1b**) or sheets (**5b**). Moreover, O–H···O and weaker C–H···O contacts also contribute moderately to the structure formation, while bromo involved interactions are very minor, although the bromine atom of the respective molecules is in a favorable peripheral position for an intermolecular contact. Nevertheless, it is obvious from the results of this study that sheets, similar to β-sheets known as an important peptide secondary structure, are formed neither in the case of the present amino acid nor dipeptide derivatives. Only the tripeptide derivative **5b** shows a corresponding structural motif in the solid state. Hence, if β-sheet formation is intended to be used in the design and construction of solid bioconjugates [34] and other bio-inspired hybrid materials including hydrogen bonded organic framework structures [2], a lower limit of at least two peptide bonds seems necessary.

## Appendix A. Supplementary data

Supplementary material available Table SUP-1: Summary of crystallographic data and refinement details for the compounds studied. Table SUP-2: Selected torsion angles (°) for compound **5b**. IR spectroscopic data. The crystal structure data for this paper have been deposited to the Cambridge Structural Database (CSD) and can be obtained free of charge at www.ccdc.cam.ac.uk/data_request/cif [or from the Cambridge Crystallographic Data Centre (CCDC), 12 Union Road, Cambridge CB2 1EZ, UK; fax: +44 (0)1223 336033; e-mail: deposit@ccdc.cam.ac.uk], quoting the CCDC deposition numbers 799300 (**1a**), 799301 (**1b**), 799302 (**3a**), 799303 (**3b**), 799304 (**4a**), 799305 (**4b**) and 799306 (**5b**). Supplementary data associated with this article can be found, in the online version, at doi:10.1016/j.molstruc.2011.03.058.

## References

[1] R.V. Ulijn, D.N. Woolfson, Chem. Soc. Rev. 39 (2010) 3349–3350.
[2] S. Toksöz, M.O. Guler, Nano Today 4 (2009) 458–469.

[3] A.J. de Graaf, M. Kooijman, W.E. Hennink, E. Mastrobattista, Bioconjugate Chem. 20 (2009) 1281–1295.
[4] M.A. Gauthier, H.-A. Klok, Chem. Commun. (2008) 2591–2611.
[5] A. de Meijere, F. Diederich, (Eds.), Metal-catalyzed cross-coupling reactions, second ed., vol. 1-2, Wiley-VCH, Weinheim, 2004.
[6] J.E. Moses, A.D. Moorhouse, Chem. Soc. Rev. 36 (2007) 1249–1262.
[7] S. Takahashi, Y. Kuroyama, K. Sonogashira, N. Hagihara, Synthesis (1980) 627–630.
[8] S. Bräse, C. Gil, K. Knepper, V. Zimmermann, Angew. Chem., Int. Ed. Engl. 44 (2005) 5188–5240.
[9] Y. Yokoyama, T. Yamaguchi, M. Sato, E. Kobayashi, Y. Murakami, H. Okuno, Chem. Pharm. Bull. 54 (2006) 1715–1719.
[10] S. Bittner, R. Scherzer, E. Harlev, Amino Acids 33 (2007) 19–42.
[11] R. Jain, B. Avramovitch, L.A. Cohen, Tetrahedron 54 (1998) 3235–3242.
[12] R. Zeynek, Hoppe Seyler's Z. Physiol. Chem. 144 (1925) 246–254.
[13] T.J. McCord, D.R. Smith, D.W. Winters, J.F. Grimes, K.L. Hulme, L.Q. Robinson, L.D. Gage, A.L. Davis, J. Med. Chem. 18 (1975) 26–29.
[14] W. Franek, Monatsh. Chem. 127 (1996) 895–907.
[15] J. Li, Y. Sha, Molecules 13 (2008) 1111–1119.
[16] A. Klages, O. Haack, Ber. Dtsch. Chem. Ges. 36 (1903) 1646–1649.
[17] H. Oelschläger, A. Seeling, M. Radman, H. Bockhard, Pharmazie 55 (2000) 825–828.
[18] Bruker, SAINT, SADABS, Bruker AXS Inc., Madison, Wisconsin, USA, 2007.
[19] G.M. Sheldrick, Acta Crystallogr., Sect. A: Found. Crystallogr. A64 (2008) 112–122.
[20] A.L. Spek, Acta Crystallogr., Sect. D: Biol. Crystallogr. D65 (2009) 148–155.
[21] W. König, R. Geiger, Chem. Ber. 103 (1970) 788–798.
[22] W. Voelter, A. Altenburg, Liebigs Ann. Chem. (1983) 1641–1655.
[23] D.A. Hoogwater, M. Peereboom, Tetrahedron 46 (1990) 5325–5332.
[24] J.R. Rachele, J. Org. Chem. 28 (1963) 2898.
[25] J. Bernstein, R.E. Davis, L. Shimoni, N.-L. Chang, Angew. Chem., Int. Ed. Engl. 34 (1995) 1555–1573.
[26] G.R. Desiraju, T. Steiner, The Weak Hydrogen Bond (IUCR Monographs on Crystallography), vol. 9, Oxford University Press, Oxford, 1999.
[27] G.R. Desiraju, in: J.L. Atwood, J.W. Steed (Eds.), Encyclopedia of Supramolecular Chemistry, Marcel Dekker, New York, 2004, pp. 658–665.
[28] G.A. Jeffrey, An introduction to hydrogen bonding, Oxford University Press, Oxford, 1997 (Chapter 2).
[29] M.C. Etter, Acc. Chem. Res. 23 (1990) 120–126.
[30] V.R. Pedireddi, D.S. Reddy, B.S. Goud, D.C. Craig, A.D. Rae, G.R. Desiraju, J. Chem. Soc., Perkin Trans. 2 (1994) 2353–2360.
[31] F.F. Awwadi, R.D. Willett, K.A. Peterson, B. Twamley, Chem. Eur. J. 12 (2006) 8952–8960.
[32] L. Brammer, E.A. Bruton, P. Sherwood, Cryst. Growth. Des. 1 (2001) 277–290.
[33] G.A. Jeffrey, W. Saenger, Hydrogen Bonding in Biological Structures, Springer, Berlin, 1991 (Chapter 19).
[34] E. Gazit, Chem. Soc. Rev. 36 (2007) 1263–1269.